IOP Conf. Series: Materials Science and Engineering **245** (2017) 022003 doi:10.1088/1757-899X/245/2/022003

Numerical Investigation of the Optimal Construction Sequence of an Actual Super Shallow Large-Span Tunnel

Zheng Zhou[1], Jiang Li[2], Bao Jin[2], Yang Liu[1]

[1] School of Transportation Science and Engineering, Harbin Institute of Technology, Harbin, China, 150090
[2] Jinan Urban Construction Group Co., Ltd, Jinan, China, 250000

zhouzhengra@163.com

Abstract. The construction process of super shallow large-span tunnel is quite complicated comparing with the construction technique of regular tunnels; therefore, it is deserved to investigate the optimal construction sequence which determines the schedule and safety management of the tunnel excavation. To address this issue, the optimal excavation procedure of the super shallow large-span tunnel is investigated using numerical analysis in this study, based on a practical tunnel project. First, the analytical finite element model of an actual tunnel structure is established to implement the numerical simulation of different tunnel excavation. Second, some numerical results are analyzed for the selection of the optimal construction excavation, such as the variation rules of the surface settlement, crown displacement and side wall deformation etc. The analytical results show that the ground surface heaves with the tunnel excavated and the crown displacement improves gradually. Finally, the optimal excavation scheme is determined by comparing the deformation of the tunnel structure and the law of surface subsidence.

1. Introduction

Owing to the complexity of construction process [1], the construction of super shallow large-span tunnel always induces the remarkable effects on the stability and integrity of surrounding structures. To reduce the above effects, several construction methods are investigated, such as the shallow buried excavation method, the shield method etc. Among the popular construction techniques, the shallow buried excavation method is widely accepted due to its flexibility for different geological conditions. In this study, the optimal construction sequence of shallow buried excavation technique is investigated by addressing the construction issue of an actual super shallow large-span tunnel.

The simulation of construction process of tunnels is greatly simplified and improved by importing the numerical method into the analysis of tunnel construction. Panet [2] proposed a method to simulate the stress variation of surrounding rock in the tunnel excavation using the release coefficient, and this approach promotes the application of numerical analysis to the tunnel construction. Yoshimura [3] validated the feasibility of finite element method by comparing the measured data with the simulation results. Recently, FEM has become the most commonly used numerical methods in tunnel excavation, and most calculation software is developed based on FEM, such as ANSYS, ABAQUS, etc. In this study, ANSYS is chosen to simulate the construction process.

2. Application to the tunnel model

2.1. Basic hypothesis of the numerical model

The numerical method is based on the following basic hypotheses [4], which simplify the practical problem to a certain extent.
(i). The surrounding rock is regarded as elastoplastic, homogeneous and isotropic material.
(ii). The time effect of the rock deformation and the influence of groundwater are neglected.
(iii). The stress and deformation of tunnel and surrounding rock are considered as plane problems.

2.2. Geometry and numerical parameter

Figure 1 shows the geological conditions of the tunnel model. The tunnel is covered with two different fills and the limestone stratum lies beneath the tunnel.

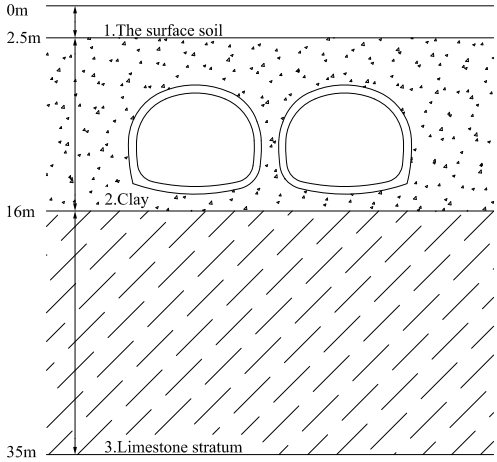

Figure1. The profile of the tunnel model

Table 1 summarizes the characteristics of the lining and the geomaterial, as it shows, the soils of homogeneous layer are provided with different characteristics. The lining is assumed to be governed by a linear-elastic behaviour with Young's modulus E = 32,500 MPa and a Poisson's ratio v = 0.2.

Table 1. Properties of geomaterial used in the tunnel model

Geomaterial	E (MPa)	c'(kPa)	φ (°)	v	γ (kN/m^3)
Surface soil	4	10	12	0.3	18.5
Sand	80	0	20	0.35	20
Limestone	300	100	22	0.45	22
Lining	32500	/	/	0.3	25

2.3. Comparison of the excavation schemes

The main construction procedures of the excavation schemes are displayed in the following pictures. It shows an apparent but slight difference among the schemes, which can influence the outcome of the analysis.

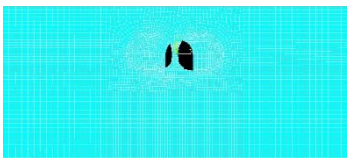
i). Construction of middle pilot heading and mid-partition wall

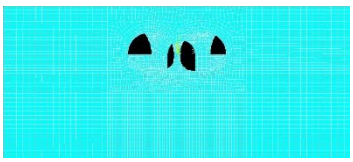
ii). Excavation of right and left pilot heading (up-step)

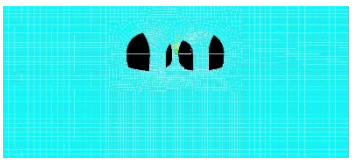
iii). Excavation of right and left pilot heading (down-step)


iv). Excavation of right and left main tunnel (up-step)

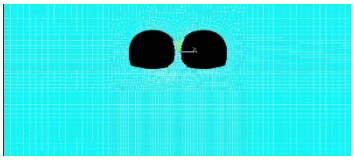
v). Excavation of right and left main tunnel (down-step)

Figure 2. The construction procedure of the excavation scheme A

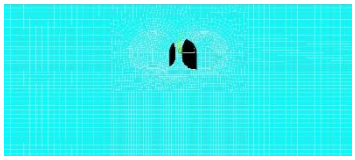
i). Construction of middle pilot heading and mid-partition wall

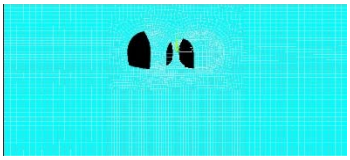
ii). Excavation of left pilot heading

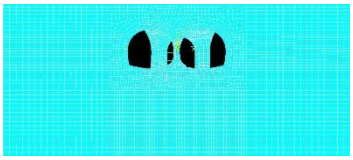
iii). Excavation of right pilot heading

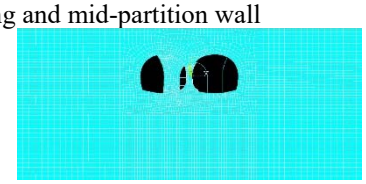
iv). Excavation of right main tunnel

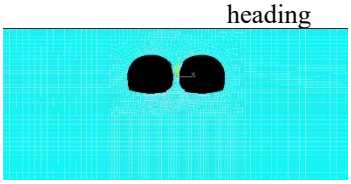
v). Excavation of left main tunnel

Figure 3. The construction procedure of the excavation scheme B

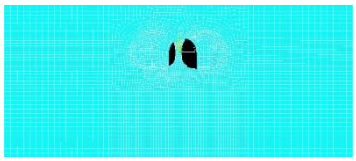
i). Construction of middle pilot heading and mid-partition wall


ii). Excavation of right and left pilot heading (up-step)

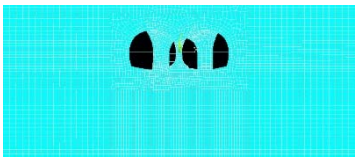
iii). Excavation of right and left pilot heading (down-step)

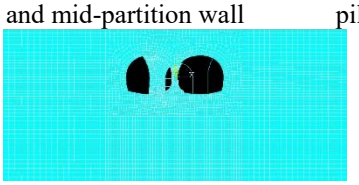
iv). Excavation of right main tunnel

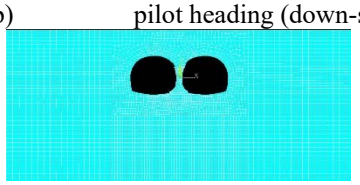
v). Excavation of left main tunnel

Figure 4. The construction procedure of the excavation scheme C

The main construction procedures are displayed above, in addition, when excavating the pilot heading, it is divided into the construction of the up step and the down step. Thus, specifically, scheme A is more efficient than the other two.

2.4. Finite element mesh

The finite element mesh can be seen in figure 2, figure 3 and figure 4. The mesh consists of 4609 planar 4-nodes isoparametric elements which contains 4720 nodes, while the lining is simulated by beam element. The size of the grid is based on the principle that the element near the structure is more intensive [5].

2.5. Calculation process

Computation is carried out in different steps according to the construction schemes, using the following parameter for the tunnel excavation: ratio of stress release $\alpha = 0.4$. In the very beginning, the model is applied with boundary conditions and initial geostress field to analyses the initial settlement and stress [6].

3. Results and discussions

3.1. The displacement of the key points

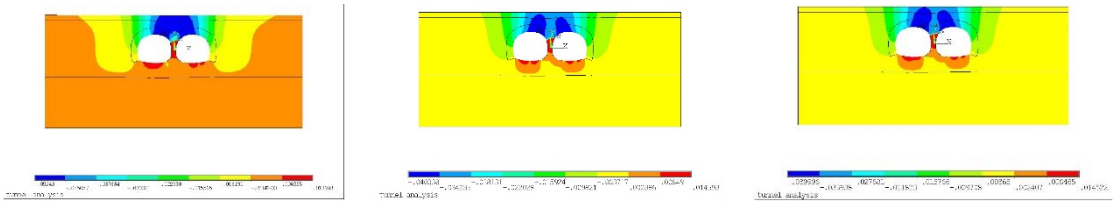

i). Scheme A ii). Scheme B iii). Scheme C

Figure 5. The diagram of final displacement (vertical)

Table 2. The displacement of the key points (vertical)

Scheme	Left crown (cm)	Right crown (cm)	Left bottom (cm)	Right bottom (cm)
A	-5.03	-4.93	1.08	1.10
B	-4.03	-3.83	1.18	1.11
C	-5.00	-4.82	1.34	1.10

Figure 5 shows the variation rules of the crown displacement and ground surface heave. The displacement of the key points is displayed in the table 2, it's seen that scheme B is with the best performance in displacement analysis. The maximal crown displacement is 5.03 cm, while the maximal bottom heave achieves 1.34 cm, besides all the values are within the displacement limit.

3.2. The stress field

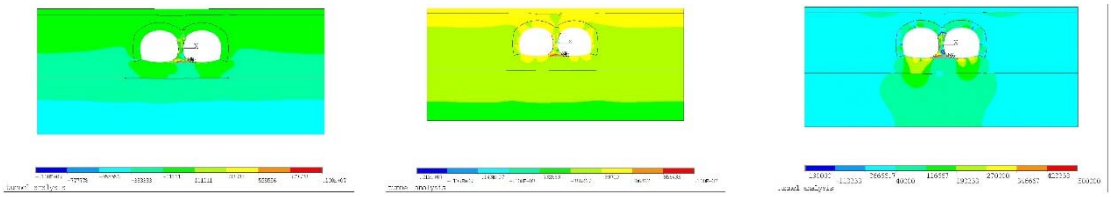

i). Scheme A ii). Scheme B iii). Scheme C

Figure 6. The diagram of first principal stress

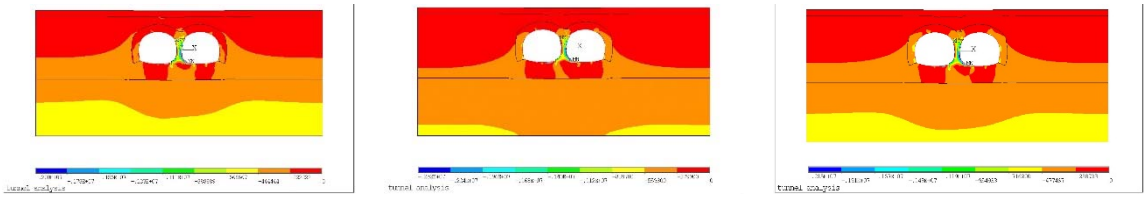

i). Scheme A ii). Scheme B iii). Scheme C

Figure 7. The diagram of third principal stress

Table 3. The first principal stress of the key points

Scheme	Left crown (MPa)	Right crown (MPa)	Left bottom (MPa)	Right bottom (MPa)
A	0.08	0.06	-0.18	-0.19
B	0.05	0.03	-0.24	-0.22
C	0.03	0.02	-0.27	-0.23

Table 4. The third principal stress of the key points

Scheme	Left crown (MPa)	Right crown (MPa)	Left bottom (MPa)	Right bottom (MPa)
A	-0.23	-0.26	-0.48	-0.40
B	-0.18	-0.15	-0.41	-0.42
C	-0.25	-0.28	-0.49	-0.47

Based on Saint Venant's Principle, it can be seen the boundary stress is hardly influenced by the tunnel [7]. Specifically, the principle stress is quite small in the present case. Obviously, the results of all the three schemes make little difference.

3.3. The internal forces of the lining

Table 5. The internal forces of the lining

Scheme	Bending moment (kN·m)		Shear force (kN)		Axial force (kN)	
	Max	Min	Max	Min	Max	Min
A	183.56	-20.39	358.36	30.54	1200	129.37
B	194.23	-21.58	308.57	12.77	1330	110.40
C	230.25	-25.58	401.68	56.87	1320	87.88

Seen from table 5, the internal forces of scheme C rank the maximum, while the scheme A is almost the same as scheme B.

4. Conclusions

The super shallow large-span tunnel is analysed using the numerical method. Three different excavation schemes are compared and discussed in detail, and the following conclusions are drawn.

(i) All the three schemes meet the requirements of the specification.

(ii) Although the three schemes are similar for the simulating the excavation procedure of an actual tunnel, the variation of deformation of structure are quite different as the processing of tunnel excavation.

(iii) Scheme B is with the best performance in displacement control, while all the three schemes perform nearly the same in stress control. For the analysis of internal forces of the lining, the results obtained by scheme C is uneconomic comparing with another two schemes.

(iv) Scheme A is determined as the optimal scheme by evaluating the efficiency of three schemes.

Acknowledgment

This study is supported by the Heilongjiang Provincial Natural Science Foundation (Grant No: E080509) and the Ministry of Housing and Urban-rural Development of China (Grant No: 2016-K4-068 and 2015-K5-014).

Reference

[1] H. Mroueh, I. Shahrour, "A simplified 3D model for tunnel construction using tunnel boring machines," *Tunnelling and Underground Space Technology*, vol. 23, pp. 38–45, 2008.

[2] Marc Panet, "Rock Mass Reinforcement by Passive Anchors," *International Conference on Anchoring &Grouting towards the New Century*, pp. 6–12, 1999.

[3] Yoshimura H., Yuki T., Yamada Y. and Kokubon N., "Analysis and monitoring of miyana railway tunnel constructed using the New Austrian Tunnelling Method," *Rock Mech. Sci.&Geomech*, vol. 23, pp. 67–75,1986.

[4] Jian Shi, Wei Ding and Shi Zhao, "Numerical simulation and analysis of tunnel excavation," *Railway Engineering*, vol. 2, pp. 21–24, 2010.

[5] Liszka T., Orkisz J., "The finite difference method at arbitrary irregular grids and its application in applied mechanics," *Computers & Structures*, vol. 11, pp. 83–95, 1980.

[6] Fakhimi A., Salehi D. and Mojtabai N., "Numerical Back Analysis for Estimation of Soil Parameters in the Resalat Tunnel Project," *Tunnelling & Underground Space Technology*, vol. 19, pp. 57-67, 2004.

[7] S.L. Crouch, A.M. Starfield and F.J. Rizzo, "Boundary element methods in solid mechanics," *Journal of Applied Mechanics*, vol. 50, pp. 96–97, 1983.